NATIONAL ADVISORY COMMITTEE FOR AERONAUTICS

TECHNICAL NOTE

No. 1492

AN INVESTIGATION OF FRETTING CORROSION UNDER SEVERAL CONDITIONS OF OXIDATION

By B. W. Sakmann and B. G. Rightmire

Massachusetts Institute of Technology

Washington

June 1948

NATIONAL ADVISORY COMMITTEE FOR AERONAUTICS

TECHNICAL NOTE NO. 1492

AN INVESTIGATION OF FRETTING CORROSION UNDER SEVERAL CONDITIONS OF OXIDATION

By B. W. Sakmann and B. G. Rightmire

SUMMARY

The purpose of the present research was to gain information as to the fundamental mechanism of fretting corrosion. More particularly, the specific questions to be answered were whether chemical action played an important role in fretting of metal surfaces and whether any such action would improve the corrosion resistance of the metals investigated. In order to answer these questions, tests were made with the same pairs of materials in air, in vacuum, in oxygen, and in helium under identical conditions of load and slip. With nearly all the materials tested there was less damage in vacuum than in air, and less in an inert atmosphere than in oxygen; in no case was the damage in vacuum greater than in air, although in most cases the friction force in vacuum was greater than in air.

The results of these experiments have shown that chemical action is of primary importance in fretting-corrosion effects, and oxide formation does not give any protection to the metals but rather increases the rate of wear. In most cases of fretting, wear between vibrating surfaces is of such a severe nature that any protective oxide films are abraded. Oxide layers are worn off even with those metals on which stable oxide films would be formed under less severe conditions of wear. As most of the metal oxides are extremely hard, the worn-off debris trapped between the vibrating surfaces acts as an abrasive. The severity of the damage depends on the hardness values of oxides and parent metals. If, for example, one of the metals is soft, the hard oxide fragments may be embedded in the softer metal, thus reducing the rate of wear.

INTRODUCTION

The term "fretting corrosion" is generally applied to the corrosion phenomena observed at the contact surfaces of machine parts subject to vibration. The occurrence of fretting corrosion has been pointed out and its general appearance described by several authors (references 1, 2, and 3). Fretting corrosion frequently appears on surfaces which are

intended to have no relative motion but which are associated with vibrating machinery. It may occur, for example, on the mating surfaces of a bearing race and of a shaft tightly fitted together, on splined surfaces, or on the contact surfaces of a railroad-car wheel and axle. It has been shown that some slippage, even though of the order of a microinch or perhaps less, is necessary to cause fretting. In the absence of slip there is no fretting (references 1 and 2).

The fretting-corrosion damage appears to be worse, other things being equal, the better the original fit of the surfaces. For this reason the fretting-corrosion problem is particularly serious in the aircraft and automotive industries, in which very close fits are employed on parts subject to vibration. In such cases fretting corrosion is serious for its own sake, since the tolerances are so small that the slight change in shape associated with the corrosion may render the parts useless. There is also evidence that the damaged surfaces develop fatigue cracks at a lower stress than nonfretted ones. Fretting corrosion may thus also act to lower fatigue strength as well as to cause surface damage (reference 4).

Investigators at the Massachusetts Institute of Technology, as well as in other places (references 2, 5, 6, 7, and 8), have done a large amount of work on the fretting-corrosion resistance of numerous pairs of materials. Although a great amount of experimental material has been gathered, the attempts to interpret the results in terms of the physical properties of the materials involved have met with only partial success. Because the phenomena of fretting corrosion are part of the more general problem of wear, the attempt was made herein to apply some of the conclusions reached in wear tests to the field of fretting corrosion. For instance, the results of wear tests with radioactive tracers (reference 9) seemed to indicate that a correlation existed between the solid solubility of the two materials and the amount of metal transferred between the rubbing surfaces. A correlation was accordingly sought between the results of the fretting-corrosion tests and the solubility of the two components involved. In some cases it seemed that the corrosion resistance was low for pairs of materials, the solid solubility of which was high. In other cases, however, no correlation could be established. A similar attempt was made to correlate the corrosion resistance with the recrystallization temperature of the fretting metals. This interpretation, too, was only partly successful.

Experimental investigations in this laboratory have so far been chiefly concerned with the corrosion resistance of numerous pairs of materials under dry conditions and - in a few cases - when lubricated with E. P. lubricants. Besides these investigations of different materials, however, a few other parameters have also been examined. The influence of hardness of one of the two surfaces has been investigated with a combination of steel on steel. Furthermore, the influence of surface roughness has been examined with a combination of copper alloy and steel.

There was no appreciable difference between the corrosion resistance of smooth and rough copper-alloy surfaces; neither did soft and hard steels behave very differently. The conclusion was, therefore, that within the range of the investigated parameters, surface finish and hardness were of secondary importance for the corrosion resistance of the two pairs of materials investigated.

A brief summary of some of the results of these observations is given in table I, in which the different combinations are given according to three grades of high, medium, and low corrosion resistance. These results are all qualitative, since the only means of evaluation so far developed is visual inspection of the specimens. Attempts have been made to measure the weight loss of the specimens, but the damaged areas are so small in the apparatus used that these attempts have been unsuccessful. From inspection of table I it is evident that none of the explanations mentioned is capable of adequately interpreting these results. It was, therefore, decided to attack the problem from a different angle, as follows.

In the general problem of wear, the role of oxidation has been a controversial subject for a long time. Fink (reference 10), for instance, believes that oxidation accelerates the wear process. This opinion is based on experiments in which wear-test specimens showed a greater weight loss in an atmosphere containing oxygen than in a chemically inert gas. Rosenberg and Jordan (reference 11), on the other hand, showed that, in some cases, oxide films on the wear-test specimens might protect the wearing surfaces. Their experiments seem to indicate that the rate of wear may be less in oxygen than in an atmosphere free of oxygen. These two sets of results suggest that sometimes oxide films give effective protection to the wearing surfaces, whereas in other cases oxidation accelerates the rate of wear. In order to protect the rubbing surfaces effectively, it is, of course, necessary that the oxide films adhere well to the surfaces of the wearing metals. Whether oxide formation has a beneficial or a detrimental influence on the wear properties depends not only on the nature of the materials involved but on the type of wear as well.

It thus appears that a knowledge of the role played by oxidation in the fretting of metal surfaces might lead to a better understanding of the fundamental processes involved in fretting corrosion. At the time when the present work was undertaken, however, only a few data were available from which any such knowledge could be gleaned. It was decided, therefore, to make tests in air and vacuum and in oxygen and helium, with the expectation that the results would shed some light on the importance of oxidation in fretting corrosion.

This work was conducted at the Massachusetts Institute of Technology under the sponsorship and with the financial assistance of the National Advisory Committee for Aeronautics.

EXPERIMENTAL APPARATUS

Vibratory System

The apparatus used for the tests the results of which are given in table I consisted essentially of a steel bar, $\frac{3}{8}$ inch by 1 inch in cross section, mounted as a horizontal cantilever beam 10 inches long. The free end of this beam was set into horizontal forced vibration at 120 cycles per second by means of a small electromagnet operated from the 60-cycle power line. A small vertical steel pillar 1 inch in length was attached to the side of the cantilever at a point 8 inches from the free end. A test specimen 1/4 inch long and 1/4 inch in diameter was attached to the upper end of the pillar; the flat top surface of this cylindrical specimen was metallographically polished. The other test specimen, which was spherical, was mounted at one end of a horizontal arm by means of which the sphere was rigidly held. It was pressed downward against the flat surface of the other specimen with any force desired by means of adjustable weights.

When the cantilever was set into vibration the cylindrical specimen tended to move back and forth in contact with the stationary sphere. The pillar to which the cylinder was attached was somewhat flexible, however, so that for small amplitudes of vibration there was no relative motion of the contacting surfaces. At a certain amplitude the static-friction force was exceeded and slip occurred. Both the absolute displacement of the cylinder and its displacement relative to the point of the cantilever at which the pillar was attached were measured by means of piezoelectric crystal pickups suitably mounted on the apparatus. The output from the pickup registering absolute displacement was fed to the horizontal-deflection plates of a cathode-ray oscilloscope, while that of the relative-displacement pickup went to the vertical-deflection plates. Since the pillar deflected elastically relative to the cantilever, the vertical motion of the cathode-ray beam was proportional to the friction force between the specimens. A force-displacement diagram thus appeared on the oscilloscope screen.

This apparatus was not used in the present tests primarily because of its size, which would have necessitated a very large vacuum chamber. Furthermore, the path of the cylindrical specimen was not a straight line but was a complicated curve, the shape of which depended on the amount of slip. A new vibratory apparatus was therefore constructed which was satisfactory in both these respects. This apparatus is shown in figure 1. The principle of operation was the same as in the previous equipment. The vibrating member D was a T-shaped piece of steel mounted on stiff flat springs K clamped to a steel base block E. The cylindrical specimen A was screwed to a flexible pillar B which

was carried by the vibrating member D. The spherical specimen C was mounted in arm G supported by springs H.

When the electromagnet F was excited with 60-cycle current, the member D was caused to vibrate at 120 cycles per second and the cylindrical specimen A tended to move back and forth in a straight line in contact with the sphere C. The absolute motion of A (i.e., the motion with respect to C) was measured by pickup I, while the motion of A relative to D was measured by pickup J. The pillar B being elastic, the latter motion was proportional to the friction force acting between the two specimens. In use, the apparatus shown in figure 1 was mounted on a circular cast-iron plate and covered with a glass bell jar.

It was considered desirable to remove as much oxygen as possible from the contacting surfaces of the specimens. This was done by electrically insulating the specimens from each other, holding them apart about 1/16 inch, and passing an electric discharge between them when the bell jar was partly evacuated. An electromagnetic device (not shown in fig. 1) which could be operated with the bell jar in place was arranged to bring the specimens into contact after the discharge had done its work and a test was to be started.

It has been pointed out that the motion and the frictional force between the two samples were measured with piezoelectric pickups. The output of the force pickup was connected to the vertical plates of a cathode-ray oscilloscope, while the displacement pickup was connected to the horizontal plates. Figure 2(a) shows a force-displacement loop as observed on the screen of the cathode-ray oscilloscope. For small amplitudes of the vibrating system an ellipse appeared on the screen. As the amplitude was increased, the ellipse became wider and higher until it suddenly assumed the shape of figure 2(a). The transition from ellipse to loop could also be effected by a decrease in the normal load pressing the specimens together. Again the transition was abrupt. This sudden change in the shape of the force-displacement diagram is interpreted as denoting the occurrence of slip between the specimens. The ellipse corresponds to purely elastic displacements, while the loop of figure 2(a) includes both elastic motion and slip. At point 1 the friction force is a maximum, corresponding to the coefficient of static friction. Between points 1 and 2, slip occurs and the friction force decreases. At point 2 the motion of the vibrating member reverses and there is no further slip until the force reaches a maximum in the opposite direction at point 3. This interpretation of the force-displacement curves is verified by the fact that no damage to the specimens occurred for an elliptical diagram. On the other hand, damage never failed to appear for a diagram like figure 2(a). It thus seems certain that slip is absent in the elliptic case but present in the other.

Figure 2(b) shows the force-time curve for the slip loop of figure 2(a); corresponding points on the two curves are denoted by the same number.

This particular shape of force curve can readily be explained. The friction force has a maximum at point 1 corresponding to the coefficient of static friction. Once the two corrosion samples start to move relative to each other the value of the friction force falls off from point 1 to point 2, at first rapidly and then more gradually. When the vibrating part reverses its direction, the friction force changes its sign and assumes a maximum value in the other direction until the specimens start to move relative to each other. Once the samples start to slip, the friction force decreases to a value corresponding to the coefficient of kinetic friction.

The displacement-time curve shown in figure 2(c) is numbered to correspond with figures 2(a) and 2(b). On comparing figures 2(c) and 2(a), it is seen that during slip, between points 1 and 2, the velocity of displacement reaches its maximum value. At point 2 the displacement is a maximum and the velocity is zero. Between points 2 and 3, where the displacement is elastic, the velocity is less in absolute value than during a slip.

As a rule most of the loops observed were not as smooth as the one shown in figure 2(a). The loops of the type shown in figure 3(a) were due to stick-slip between the corrosion specimens. During the slip period the specimens do not slide uniformly but the motion is an intermittent sliding and sticking. At point 1 of the loop the friction force corresponds to the static-friction coefficient. As the samples start to slide, the friction force decreases, but at point 1' of the loop the specimens stick again and the friction force increases. The same process repeats itself at point 1''. The three successive maximums of the friction force become more evident from inspection of the force-time curve of figure 3(b). The displacement-time curve is shown in figure 3(c). Corresponding points of figures 3(a), 3(b), and 3(c) are denoted by the same numbers. It will be noted that the horizontal parts of the displacement-time curve of figure 3(c) correspond to the periods of rest in the stick-slip cycle.

Vacuum System

The vacuum system was designed in such a way that it was possible to exchange the fretting-corrosion specimens quickly and easily. A bell-jar system fulfilled these requirements, although the vacuum attainable was limited by the inevitable leaks between bell jar and base plate. A schematic diagram of the whole system is shown in figure 4. In this figure, 25-millimeter pyrex tubing is indicated by a double line and the 10-millimeter connections are drawn as single lines. The whole system was mounted underneath a table; the pump plate, which had five electric lead-ins, was permanently screwed to the top of the table. One pair of connections was used for the two electrostatic pickups;

a third electrode was connected with the electromagnet exciting the vibrating system. The fourth lead-in actuated the release mechanism of the upper fretting-corrosion specimen. The fifth electrode was connected with a high-voltage transformer, which was used for producing an electric discharge between the two corrosion specimens. It was hoped that this discharge would drive out the gases which might be adsorbed on the surfaces of the samples.

A Cenco Megavac pump was used for the mechanical forepump. In the high-vacuum part of the system two mercury-vapor diffusion pumps were connected in series. The first was of pyrex glass; the second was of steel. All the main connections from mechanical pump to diffusion pumps and bell jar were made with 25-millimeter pyrex tubing to insure a speedy evacuation of the system. The connections to the steel diffusion pump were sealed with de Khotinsky cement. Initially, a large liquid-air trap was included between the steel diffusion pump and the bell jar. The connection between steel diffusion pump and this liquid-air trap was found to be a weak spot in the vacuum system. The diameter of the part of this glass trap joining the steel diffusion pump was more than 80 millimeters. It was found that small cracks in this glass gave rise to leaks. Because of the difficulty of annealing the large-diameter tubing, new cracks appeared after the old leaks were sealed. It was finally decided to discard this liquid-air trap.

McLeod gauges A and B were used to measure the pressure in the fore-vacuum and high-vacuum parts of the system, respectively. The minimum pressures which could be measured with the two gauges with any accuracy were 10^{-4} and 10^{-5} millimeters of mercury, respectively. The five stopcocks of the vacuum system, which are shown in figure 4, were arranged in such a way that they could be conveniently handled by an operator sitting in front of the table on which the apparatus was mounted.

Different seals were tried for the connection between the chromium-plated pump plate and the finely ground rim of the bell jar. It was found that the best seal was achieved when a Cenco vacuum-sealing compound was applied to the ground rim of the bell jar before it was put on the plate. After the jar was put in position an Apiezon wax was applied to the joint to give additional protection against leaks. In the course of this work two bell jars were used with volumes of about 35 liters and 18 liters.

The bell jar could be shut off from the vacuum system with 1-inch stopcock V of figure 4. The position of the stopcocks in figure 4 corresponds to normal operating conditions during the evacuation of the bell jar. After a corrosion test, stopcock V was shut, and stopcock III was turned by an angle of 90° in a clockwise direction to connect McLeod gauge B with the steel diffusion pump; air was then admitted to the bell jar by turning the three-way stopcock II by an angle of 45° in

a clockwise direction. After the corrosion specimens had been exchanged, the bell jar was put back and stopcock II was turned in such a way that the fore-pump system was connected with the bell jar (45° from the position of the stopcock in fig. 4 in a counterclockwise direction). When the pressure in the bell jar was low enough for effective operation of the diffusion pumps, stopcock V was opened. In this way air could be admitted to the bell jar without the necessity of waiting for the diffusion pumps to cool. When McLeod gauge B was directly connected with the steel diffusion pump while stopcock V was shut, McLeod gauge B showed sticking vacuum, thus indicating a pressure of 10^{-5} to 10^{-6} millimeters of mercury. The conclusion was that the system up to the 1-inch stopcock V did not contain any appreciable leaks. When the bell jar was connected with the system, the pressure was considerably higher because of the inevitable leak between bell jar and pump plate. The vacuum of the bell jar during the tests was between 10^{-5} and 5×10^{-4} millimeters of mercury. The leak rate of the bell jar was between 10 and 100 microns per hour, the rate depending on the quality of the seal between bell jar and pump plate. The speed of the steel diffusion pump was about 4 liters per second. The vacuum attained was in good agreement with the measured leak rate, the pump speed, and the volume of the system to be evacuated.

The leak between bell jar and pump plate was mentioned as the main limitation of the system. Another limitation was the amount of gas given off by the fretting-corrosion apparatus. As it was impossible to heat the bell jar, the bad effects of the gas developed could not be avoided. For a given leak rate, the maximum vacuum could be reached more quickly when the fretting-corrosion apparatus was not under the bell jar.

TEST PROCEDURE

Visual observation of the corrosion damage was the chief means used to estimate the corrosion resistance of the tested materials; furthermore the amount of debris formed during the test gave a good indication of the quality of the combination. Weighing of the specimens before and after testing was also tried. Since, however, the weight loss could be either positive or negative (on account of the chemical action at the surface) and since the weight changes were found to be too small for measurement on an analytical balance, the attempt was abandoned. Other observed factors were the height and shape of the slip loop formed on the screen of the cathode-ray oscilloscope. The average height of the loop was a measure of the magnitude of the friction force, and any changes in the shape of the loop revealed variations of the friction force during the test. The electromagnet of the vibrating system was fed through a Variac, the position of which was also recorded. This position, as well as the height of the friction loop, gave an indication of the magnitude of the friction force between the two specimens.

For any two corrosion experiments, it could readily be decided by visual inspection which test had yielded the greater amount of debris. For that reason two photographs of each corroded specimen were taken. The first photograph showed the specimen with the debris formed during the test; the second depicted the corroded spot after the debris had been wiped off the surface. In the corrosion experiments discussed in the following paragraphs, it is felt that the amount of debris gives in many cases a good indication of the relative merits of a given pair of materials tested under different experimental conditions.

In order to gain a further indication of the severity of the corrosion damage, the following procedure was frequently applied. After the corrosion experiment, the test specimen was polished with a soft cloth. The length of time required to remove the corrosion spot was taken as a measure of the corrosion damage. This test was particularly valuable in those cases in which a soft metal was rubbed against a harder surface. In these cases it often happened that no real damage was done to the hard material but some of the soft metal was smeared over the hard surface. Inspection under the microscope sometimes revealed differences in color, which were helpful in distinguishing between material transfer and damage. Unfortunately, the colors do not appear in the photographs.

The tests were divided into two groups, the first of which comprised several pairs of materials chosen from all three classes of table I so as to get a well-rounded picture of the effect of oxidation on fretting corrosion.

In the second group of tests, materials with low corrosion resistance were investigated under various conditions. Experiments were made in air, oxygen, and a chemically inert atmosphere. Moreover, with the combination of steel on steel, the influence of degassing in an electric discharge was examined in more detail. With all the other materials tested, no difference in corrosion damage could be detected between degassed test samples and the specimens used ordinarily. With steel, however, a marked difference was found.

The test conditions were chosen to be the same as those of the earlier runs for which the results are recorded in table I. These conditions were as follows:

Normal load, grams 20

Total maximum displacement of cylindrical specimen with respect to spherical specimen, millimeters. . . . . 2×10^{-2}

Duration of test, minutes. 6.0

There is some uncertainty in the value of 2×10^{-2} millimeter for the maximum displacement, but this uncertainty does not affect the comparative results reported herein, since the displacement was the same for all tests. The force-displacement curves observed for these tests were not, in general, so well formed as those shown in figures 2 and 3.

Violent fluctuations in the friction force sometimes occurred during the cycle, like the stick-slips shown in figure 3(a), but on a larger scale. Occasionally also, the motion was not steady, the shape of the diagram changing from cycle to cycle. It was possible in all cases, however, to hold the maximum displacement nearly constant throughout a run. This was accomplished by slight adjustment of the Variac.

DISCUSSION OF RESULTS

The first pair of materials to be tested in vacuum and air was a phosphor-bronze ball run against a carbon-steel flat. Figure 5(a) shows the ball after the test in the air. A large amount of debris was found, which could be wiped off without difficulty. (See fig. 5(b).) The corroded spot looked darker than the surrounding surface, thus indicating that the damaged spot was badly oxidized.

Figure 5(c) shows the corroded spot on the sphere after a test in the evacuated bell jar. In this case, the damaged spot was highly reflecting and no signs of oxidation were visible. After the test in vacuum, no debris was found on the phosphor-bronze sphere; all the few fragments formed during the test in vacuum were deposited on the steel flat. For that reason only one photograph of the sphere was taken.

Figure 6 shows the wear spots on the steel flat. In the test in the air, the major part of the fragments was deposited on the sphere; some of the oxidized fragments, however, were left on the steel flat, as can be seen in figure 6(a). The fact that after the test in vacuum the corroded spot on the steel flat had the color of the phosphor-bronze sphere indicated that some material was transferred from the sphere to the flat. During the test in vacuum, the amount of debris formed was considerably less than in air, and all of it was deposited on the steel flat shown in figure 6(c). Although the damaged area was larger in vacuum than in air, the depth of the damage and its severity were less in vacuum. (See figs. 6(b) and 6(d).) Moreover, the polishing procedure showed that part of the corrosion spots of figures 6(c) and 6(d) was material transferred from the phosphor-bronze sphere rather than damage to the surface of the steel flat.

Table I shows that the corrosion resistance of the combination of copper alloy and steel has an intermediate value. This position of copper alloy in the table can perhaps be explained by the fact that, of the different metal oxides, the hardness of copper oxide has an intermediate value of 3.5 to 4 on the Moh scale. In this particular case, the strongest indication as to the relative corrosion resistance in air and in vacuum can be gained from the amount of debris formed during the tests. Comparison of figures 5(a) and 6(c) shows that many more fragments were formed during the test in air. This fact indicates clearly that the corrosion resistance is higher in vacuum than in air.

In the next run, in which a tin hemisphere was run against a steel flat, the difference between the damage in air and in vacuum was even greater than with the preceding combination of phosphor-bronze on steel. Figures 7(a) and 7(b) show the damage to the tin hemisphere after the two tests. It is evident from figure 7(a) that this damage was very severe after the test in air. As in the preceding test with phosphor-bronze, the surface of the tin hemisphere was highly reflecting after the test in vacuum; this indicated that a clean tin surface was formed. There was no indication of any oxidation of the abraded surface after the test in vacuum. Figure 8 shows the damaged areas on the steel flat. It is evident from figure 8(a) that a large amount of debris was formed during the test in air. Only part of the fragments produced is visible in figure 8(a). Figure 8(c) shows a corroded spot of another test under the same conditions of load and slip. The debris was easily removed from the steel flat by wiping. Inspection of the damaged spots of figures 8(a) to 8(c) makes it apparent that corrosion damage was very serious. In table I the combination of tin and steel was classified as having a low corrosion resistance. This classification is in good agreement with the fact that tin oxide is considerably harder than copper oxide, having a hardness value between 6 and 7 on Moh's scale.

Figure 8(d) shows the corrosion spot after a test in vacuum. The steel surface was not damaged; the only visible effect of the test was that a certain amount of tin was transferred to the steel flat. For the test in vacuum, only one photograph was taken, as no debris was formed during this test. If the corrosion resistance of tin on steel in vacuum were classified, it would have to be placed in the column of high corrosion resistance. A comparison of figures 8(a) to 8(c) with figure 8(d) shows that the damaged area of the test in air was more than twice that in vacuum. The round shape of the corroded spot of figure 8(c) was more typical than the elongated form shown in figures 7(a), 8(a), and 8(b). The tests made with tin on steel demonstrate most clearly the influence of an oxidizing atmosphere on the corrosion resistance.

As the third pair of materials in the first group, an aluminum hemisphere was run against a flat of aluminum-silicon alloy. Table I shows that the combination of aluminum on aluminum has a low corrosion resistance. This classification is borne out by the severe damage shown in figures 9(a), 9(b), 10(a), and 10(b). This low corrosion resistance is probably due to the fact that aluminum oxide is one of the hardest metal oxides, having a hardness value of 9 on Moh's scale. After the test in air, a large amount of debris was found on both hemisphere and flat. The results of the test in vacuum are illustrated in figures 9(c), 9(d), and 10(c). It is evident that the damage under these conditions was much less severe than in air and that fewer fragments were formed.

The fourth pair of materials tested was a combination of lead on steel. On the old apparatus, it had been found that this combination had very good corrosion properties. Figures 11(a) and 11(b) show lead hemispheres after test in air and in vacuum, respectively. The corroded spot on the hemisphere run in vacuum was highly reflecting; this indicated that no oxidation took place. The corresponding spots on the steel flats are shown in figures 11(c) and 11(d). The two tests in air and in vacuum did not show any appreciable difference inasmuch as no serious damage was done to the steel flat in either case. The material transferred from hemisphere to flat under either condition could be wiped off with a cloth. Although lead oxide is rather hard, having a hardness value of 5 to 6 on Moh's scale, the combination of lead on steel has favorable properties. This is probably due to the fact that during the test the hard oxide fragments were embedded in the soft lead and were thus prevented from damaging the steel surface.

Another test was run with a steel sphere and a lead-plated steel flat, the results of which are shown in figure 12. As in the preceding test, material was transferred from lead surface to steel surface without damaging the latter, and all the transferred material could be rubbed off with a cloth. Comparison of figures 12(a) and 12(c) with figures 12(b) and 12(d) shows that the area of contact was larger in vacuum than in air. This difference might have been due to the fact that the hard lead oxide formed during the test in air made it possible for the thin lead plate to support the load over a smaller contact area.

The second group of runs was devoted entirely to pairs of materials with a low corrosion resistance and particularly to the combination of steel on steel. Because of its general importance in engineering problems, more tests were made with this combination than with any so far discussed. In one respect, the combination of steel on steel behaved differently from the other materials tested. The degassing of the specimens in an electric discharge had a pronounced influence on the corrosion resistance, but with the other materials described in this report degassing did not seem to change the corrosion resistance. For tests in vacuum with steel specimens, the damage of degassed corrosion samples was less severe under otherwise identical conditions of pressure. This point is illustrated in figures 13 and 14. Figure 13(a) shows the corroded spot on the steel sphere after a corrosion test in air under atmospheric conditions. Figure 13(b) shows the damage to the steel sphere after a test in vacuum, and figure 13(c) shows the damage to a degassed steel sphere tested in vacuum. Figure 14 shows the corresponding spots on the steel flats, which are mirror images of the spots on the spheres. Comparison of figures 13 and 14 makes it evident that the greatest amount of damage was done to the specimens run in air at atmospheric pressure, whereas the degassed specimens run in vacuum showed the least damage. Figures 15 and 16 show the same corrosion spots at different magnifications. These photographs show that not only the area of the corroded

part of the specimens was different but also the seriousness of the damage. No explanation is at hand for the fact that degassing of the test specimens in an electric discharge had a marked effect with the combination of steel on steel and none with the other materials tested.

In the next experiments, the combination of steel on steel was tested in air and oxygen at atmospheric pressure. The spots of the two tests, which were both on the same flat, are depicted in figures 17(a) and 17(b). The right-hand spot resulted from the test in air; the left-hand spot was produced by the test in oxygen. It is evident from these figures that the amount of debris formed, as well as the damage to the steel flat, was almost identical for both tests. This result is not surprising if it is noted that the partial oxygen pressures differed by only a factor of 5, whereas the corresponding factor for the tests in air and vacuum was approximately 10^7.

It seemed desirable to see whether these results could be corroborated with another pair of materials. It was decided to choose the combination of aluminum on aluminum, which had been tested before in air and in vacuum (see figs. 9 and 10). Figure 18 shows the damaged part of an aluminum hemisphere after tests in air and in oxygen at atmospheric pressure. Figure 19 shows the corresponding spots on the aluminum-silicon-alloy flats. The spots on the flats were mirror images of those on the hemispheres. The amount of debris formed during the tests and the severity of the damage were very similar for oxygen and air. It can be noted in figure 19(b) that the debris on the flat could not be wiped off readily, an appreciable part remaining after the flat had been wiped with lens paper. The corroded spots were irregular because the aluminum hemisphere was turned on a lathe and its surface was uneven. The results of the tests with aluminum corroborate those with steel, and it may be concluded in both cases that air and pure oxygen have the same corrosive properties in fretting tests.

In continuation of the second group of tests, fretting experiments were made in air and helium, both under atmospheric pressure. For the tests in helium, the bell jar was first evacuated and helium was then admitted into the system. The fretting tests in helium lasted several minutes, during which time some air leaked into the system. The leak rate was very low, however, because the pressure inside and outside the system was the same. The tests were, therefore, performed in a mixed atmosphere rich in helium but also containing some air. In examining the results of these tests, it must be remembered that the helium atmosphere was far from being free of oxygen.

Figures 20(a) and 20(b) show the damaged part of two steel balls after a corrosion test in air and helium, respectively. Because most of the debris accumulated on the flat in both tests, only one photograph

of each steel ball was taken. Figures 21(a) to 21(d) show the corresponding spots on the flats. It is evident from an inspection of figure 21(a) that a large amount of debris was formed during the test in air; figure 21(c), on the other hand, shows only very few fragments. The conclusion is, therefore, that considerably less debris is formed in helium than in air, although the helium atmosphere contained some air.

It is interesting to note that the findings in the present paper are in accord with the conclusions of Dies (references 5 and 6), wherein the phenomena of fretting corrosion are explained by the assumption that the hard particles of metal oxide which are trapped between the vibrating surfaces act as an abrasive and damage the metal surface. This mechanism seems to operate even with metals which - under less severe conditions - form stable oxide layers.

CONCLUSIONS

Tests made with the same pairs of materials in air, in vacuum, in oxygen, and in helium under identical conditions of load and slip show conclusively that oxidation plays an important role in fretting corrosion. The debris formation and the severity of the damage were considerably less in air under reduced pressure of 10^{-4} to 10^{-5} millimeters of mercury than in air at atmospheric pressure. Likewise, corrosion tests performed in an inert atmosphere produced less damage than experiments performed in air or oxygen under otherwise identical conditions.

The hardness of the oxides appears to be an important property in connection with fretting corrosion. The damage produced is large with those combinations in which both the metal and its oxide are hard. The high corrosion resistance of lead on steel can be explained by the fact that the hard oxide particles embed themselves in the soft lead and hence do comparatively little damage. It can thus be concluded that fretting corrosion belongs to the group of wear problems for which oxidation affords no protection.

The fact that the oxides of all metals of practical importance are hard makes the prevention of fretting-corrosion damage a difficult task. The reduction of oxidation by evacuation is ordinarily feasible only in experiments such as are described in this report. The question as to whether the access of oxygen to the fretting surfaces can be reduced by some other means, as for instance by the application of greases or lubricating oils, is outside the scope of the present investigation.

Massachusetts Institute of Technology
Cambridge, Mass., December 4, 1946

REFERENCES

1. Tomlinson, G. A.: The Rusting of Steel Surfaces in Contact. Proc. Roy. Soc. (London), ser. A, vol. 115, no. 771, July 1, 1927, pp. 472–483.

2. Tomlinson, G. A., Thorpe, P. L., and Gough, H. J.: An Investigation of the Fretting Corrosion of Closely Fitting Surfaces. Proc. Inst. Mech. Eng. (London), vol. 141, no. 3, May 1939, pp. 223–237.

3. Eden, E. M., Rose, W. N., and Cunningham, F. L.: Endurance of Metals. Proc. Inst. Mech. Eng. (London), vol. 4, Oct. 1911, pp. 839–880. (See p. 875.)

4. Warlow-Davies, E. J.: Fretting Corrosion and Fatigue Strength. Brief Results of Preliminary Tests. Proc. Inst. Mech. Eng. (London), vol. 146, no. 1, Nov. 1941, pp. 32–38.

5. Dies, Kurt: Fretting Corrosion, Chemical-Mechanical Phenomenon. The Engineers' Digest (American Ed.), vol. 2, no. 1, Jan. 1945, p. 14.

6. Dies, K.: Composition of Abraded Dust, Iron and Coal. Trades Rev., vol. 148, no. 3980, June 1944, pp. 866, 868.

7. Gray, H. C., and Jenney, R. W.: An Investigation of Chafing on Aircraft-Engine Parts. SAE Jour., vol. 52, no. 11, Nov. 1944, pp. 511–518.

8. Sachs, G., and Stefan, P.: Chafing Fatigue Strength of Some Metals and Alloys. Trans. American Soc. Metals, vol. 29, no. 2, June 1941, pp. 373–399.

9. Sakmann, B. W., Burwell, J. T., Jr., Irvine, J. W., Jr.: Measurements of the Adhesion Component in Friction by Means of Radioactive Indicators. Jour. Appl. Phys., vol. 15, no. 6, June 1944., pp. 459–473.

10. Fink, M.: Wear Oxidation, a New Component of Wear. Trans. American Soc. Steel Treating, vol. 18, July-Dec., 1930, pp. 1026–1034.

11. Rosenberg, S. J., and Jordan, L.: The Influence of Oxide Films on the Wear of Steels. Trans. American Soc. Metals, vol. 23, no. 3, Sept. 1935, pp. 577–613.

TABLE I

FRETTING-CORROSION RESISTANCE OF VARIOUS MATERIALS UNDER DRY CONDITIONS

Corrosion resistance		
Low	Medium	High
Steel on steel	Cadmium on steel	Lead on steel
Nickel on steel	Zinc on steel	Silver plate on steel
Aluminum on steel	Copper alloy on steel	Silver plate on aluminum plate
Aluminum-silicon alloy on steel	Zinc on aluminum	Parkolubrited steel on steel
Antimony plate on steel	Copper plate on aluminum	
Tin on steel	Nickel plate on aluminum	
Aluminum on aluminum	Silver plate on aluminum	
Zinc-plated steel on aluminum	Iron plate on aluminum	
Iron-plated steel on aluminum		

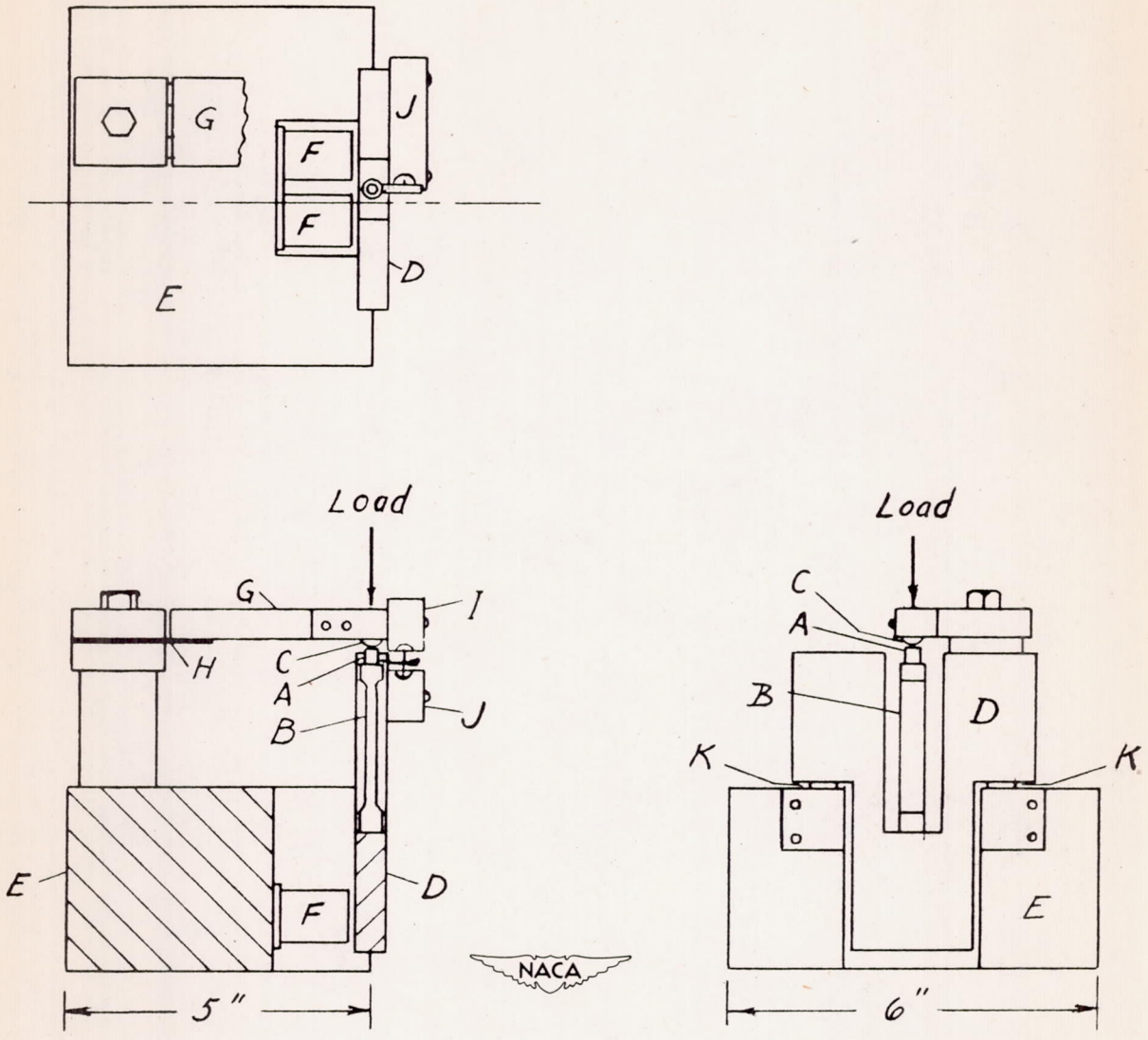

Figure 1.- Vibratory apparatus. A, cylindrical specimen; B, flexible steel pillar; C, spherical specimen; D, vibrating member; E, base block; F, electromagnet; G, arm for holding spherical specimen; H, spring-steel hinge; I, pickup for absolute displacement of cylindrical specimen; J, pickup for displacement of cylindrical specimen relative to vibrating member D (friction-force pickup); K, flat-spring supports for vibrating member D.

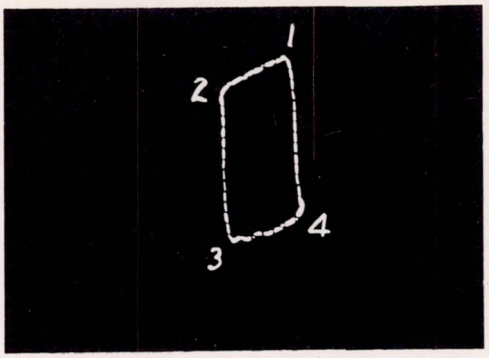

(a) Slip loop.

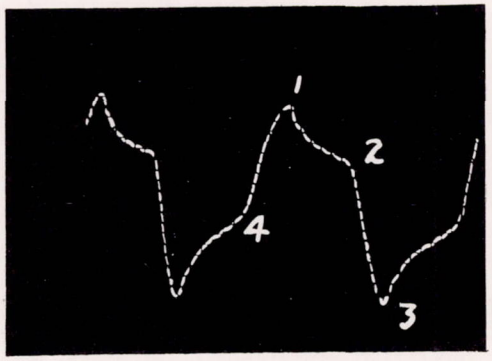

(b) Force-time curve.

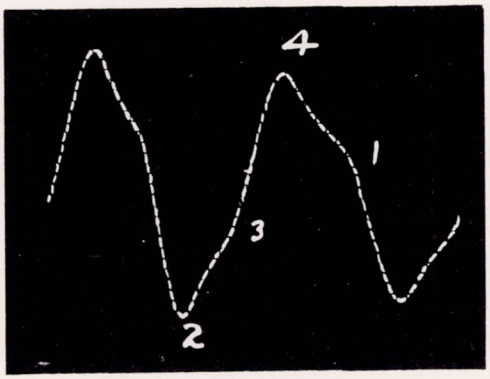

(c) Displacement-time curve.

Figure 2.- Force and displacement curves without stick-slip.

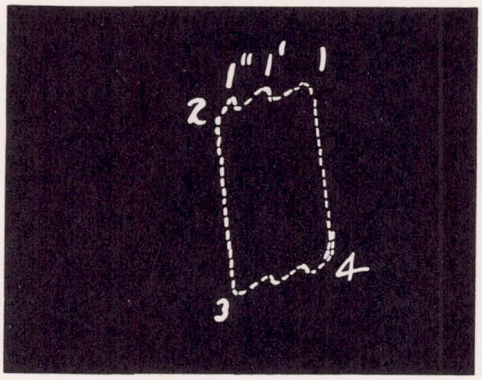

(a) Slip loop.

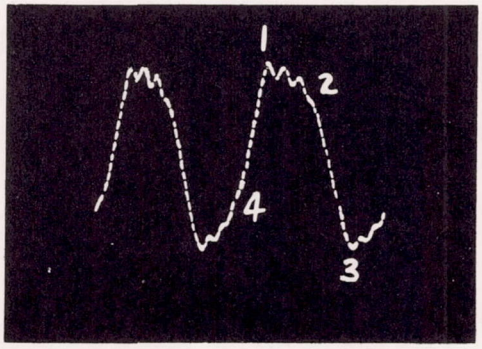

(b) Force-time curve.

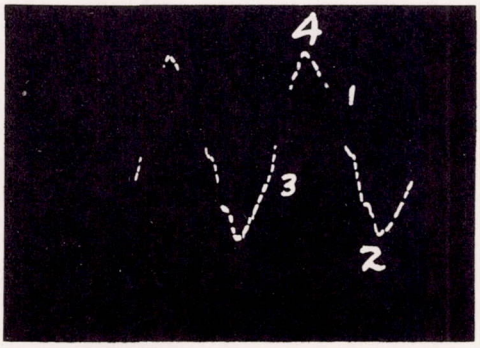

(c) Displacement-time curve.

Figure 3.- Force and displacement curves with stick-slip.

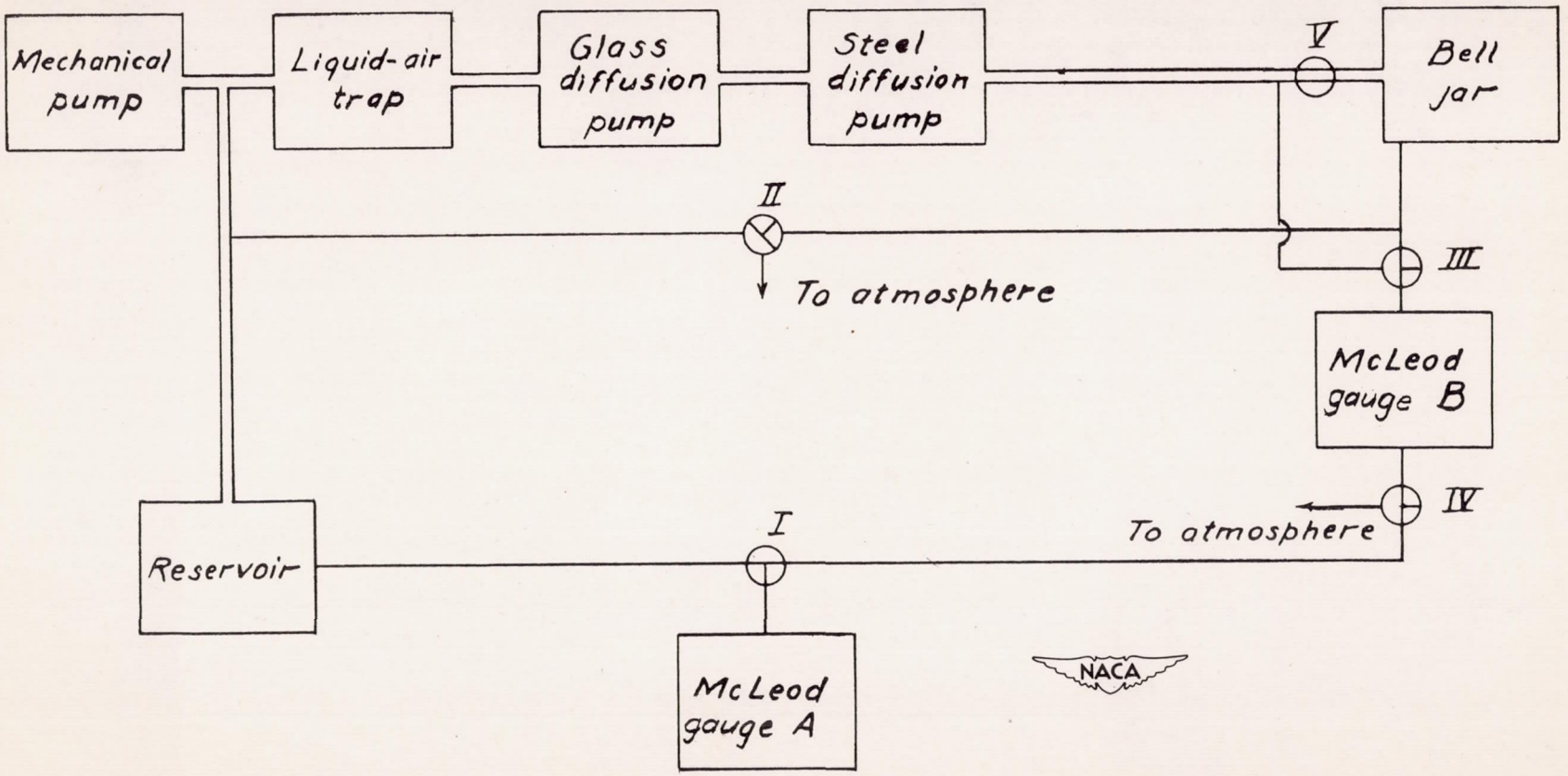

Figure 4.- Schematic diagram of vacuum system.

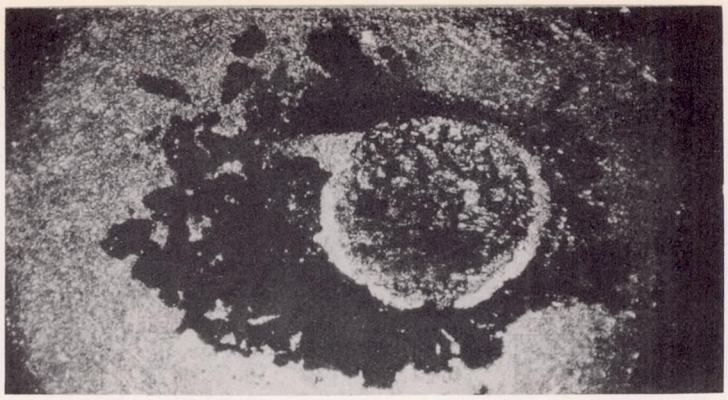

(a) Phosphor-bronze sphere after test in air of atmospheric pressure. Before wiping.

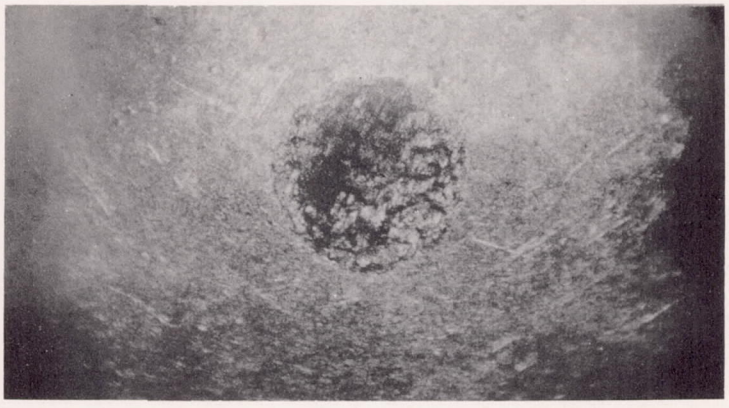

(b) Phosphor-bronze sphere after test in air of atmospheric pressure. After wiping.

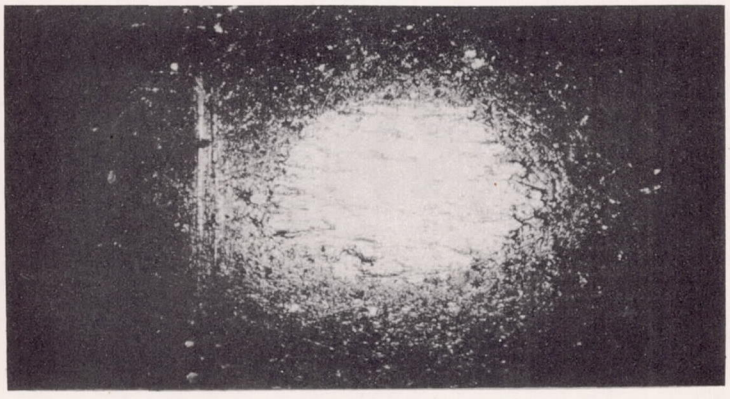

(c) Phosphor-bronze sphere after test in vacuum. Wear spot is highly polished.

Figure 5.- Phosphor-bronze sphere run against SAE 1020 steel flat in air and vacuum. Magnified 50 times.

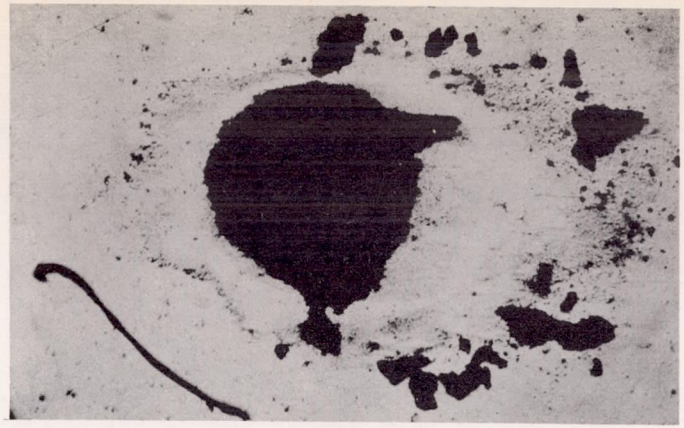

(a) Steel flat after test in air of atmospheric pressure. Before wiping. Damaged spot has color of phosphor-bronze sphere.

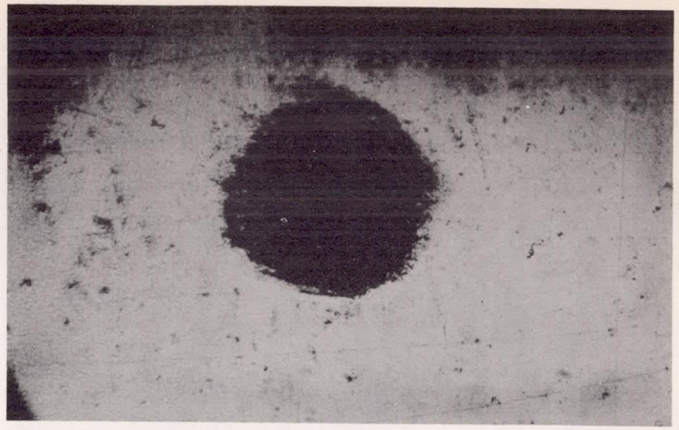

(b) Steel flat after test in air of atmospheric pressure. After wiping. Damaged spot has color of phosphor-bronze sphere.

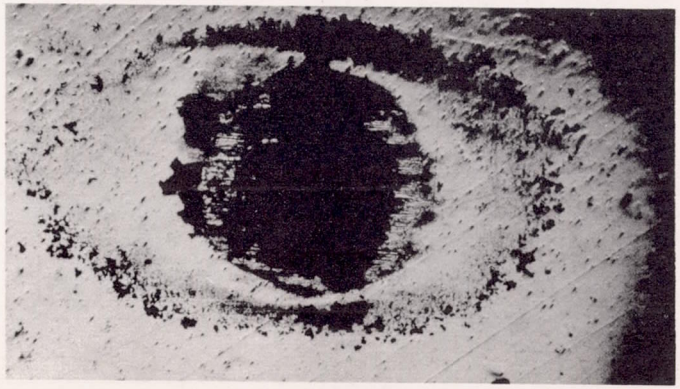

(c) Steel flat after test in vacuum. Before wiping. Damaged spot has color of phosphor-bronze sphere but to lesser extent than after test in air.

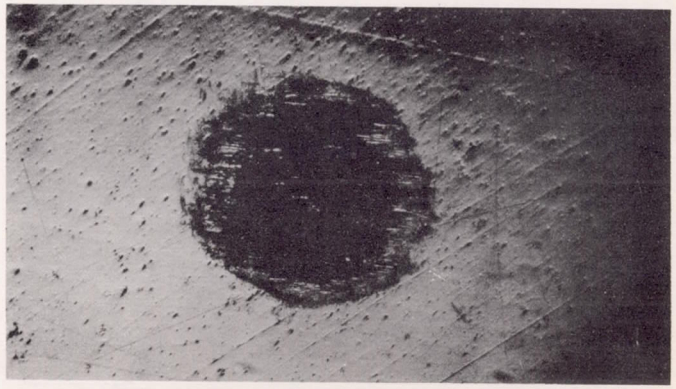

(d) Steel flat after test in vacuum. After wiping. Damaged spot has color of phosphor-bronze sphere but to lesser extent than after test in air.

Figure 6.- SAE 1020 steel flat run against phosphor-bronze sphere in vacuum and air. Magnified 50 times.

(a) Tin hemisphere after test in air of atmospheric pressure. Most of the debris is on the flat.

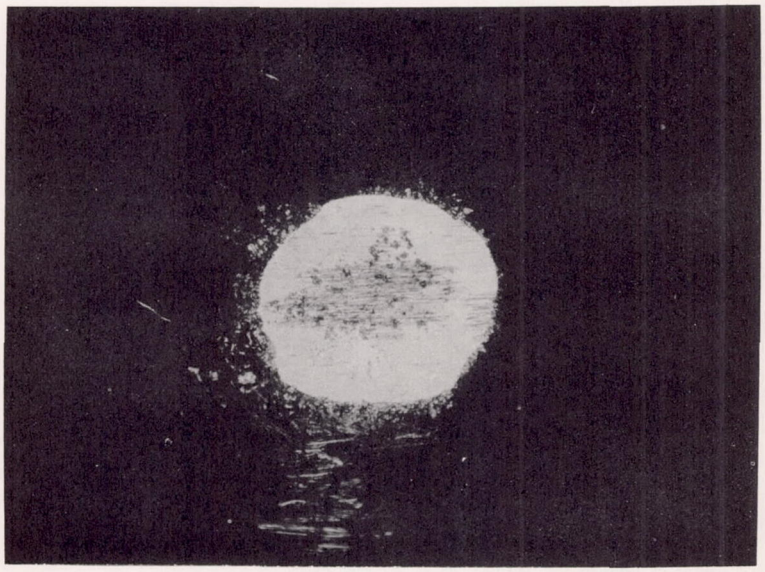

(b) Tin hemisphere after test in vacuum. Wear spot is highly polished.

Figure 7.- Tin hemisphere run against SAE 1020 steel flat in air and vacuum. Magnified 50 times.

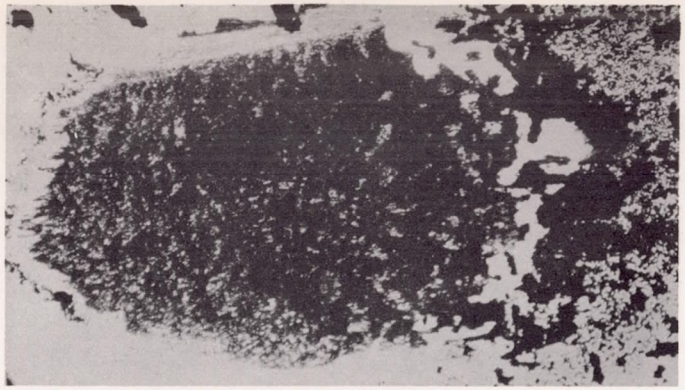

(a) SAE 1020 steel flat after test in air of atmospheric pressure. Before wiping. About 70 percent of the debris formed is shown.

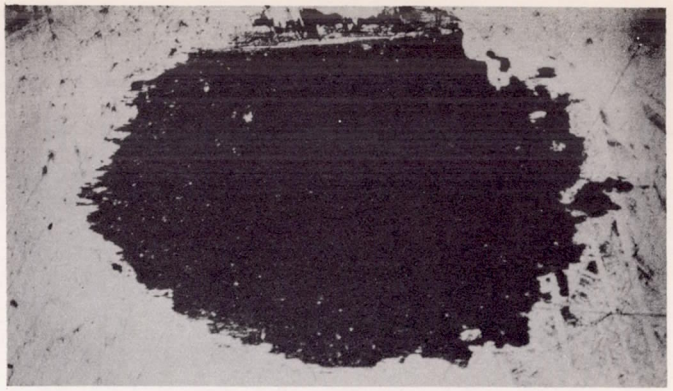

(b) SAE 1020 steel flat after test in air of atmospheric pressure. After wiping.

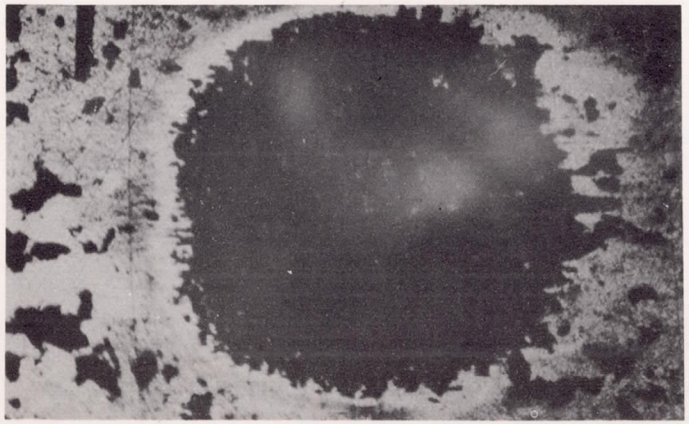

(c) SAE 1020 steel flat after test in air of atmospheric pressure.

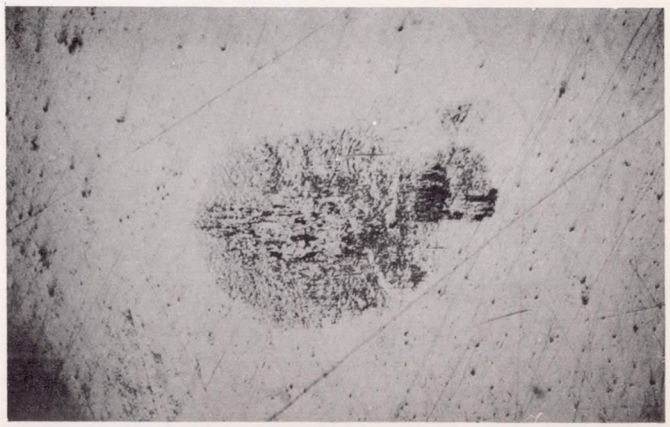

(d) SAE 1020 steel flat run against tin in vacuum.

Figure 8.- SAE 1020 steel flat run against tin hemisphere in air and vacuum. Magnified 50 times.

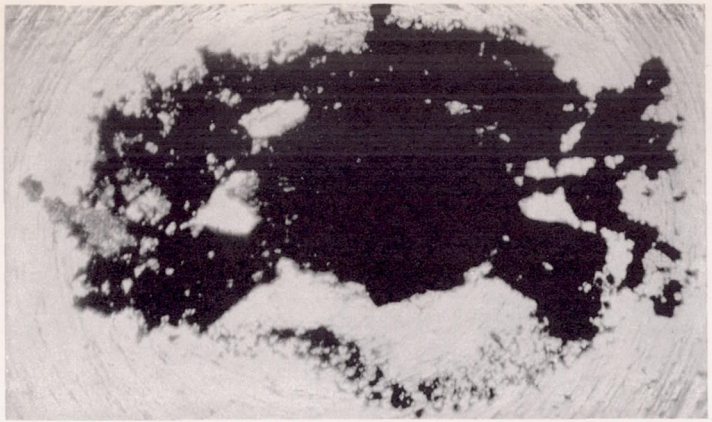

(a) Aluminum hemisphere after test in air of atmospheric pressure. Before wiping.

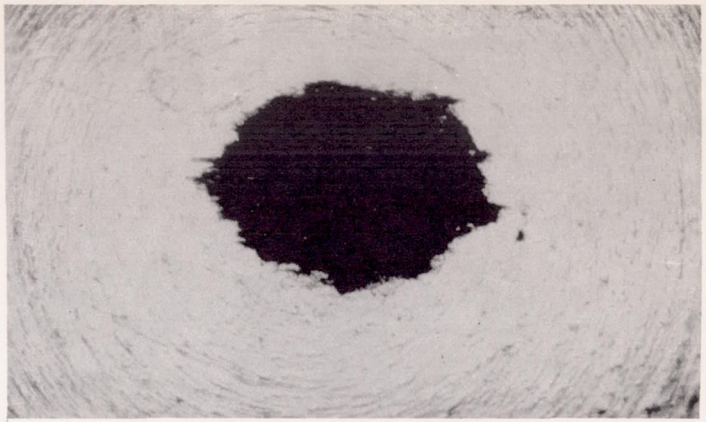

(b) Aluminum hemisphere after test in air of atmospheric pressure. After wiping.

(c) Aluminum hemisphere after test in vacuum. Before wiping.

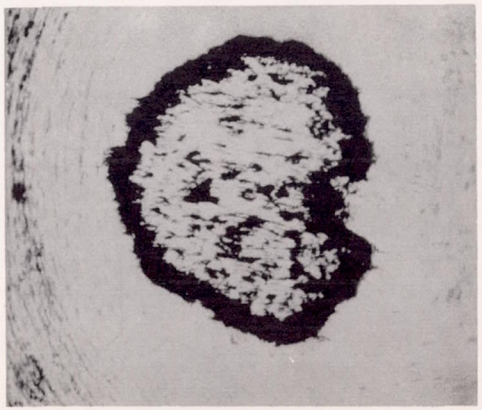

(d) Aluminum hemisphere after test in vacuum. After wiping.

ure 9.- Aluminum hemisphere run against aluminum-alloy flat in air and vacuum. Magnified 100 times.

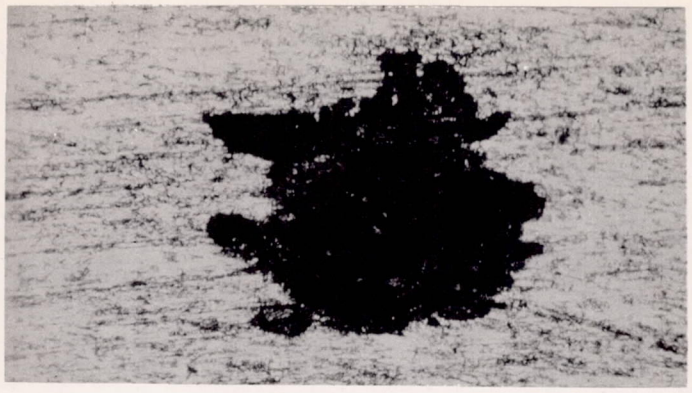

(a) Aluminum-alloy flat after test in air. Before wiping.

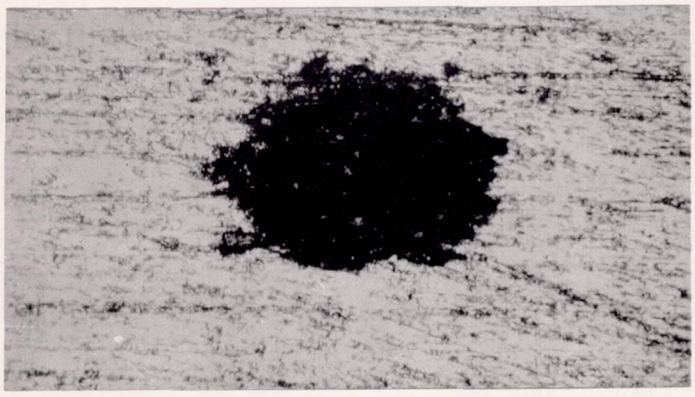

(b) Aluminum-alloy flat after test in air. After wiping.

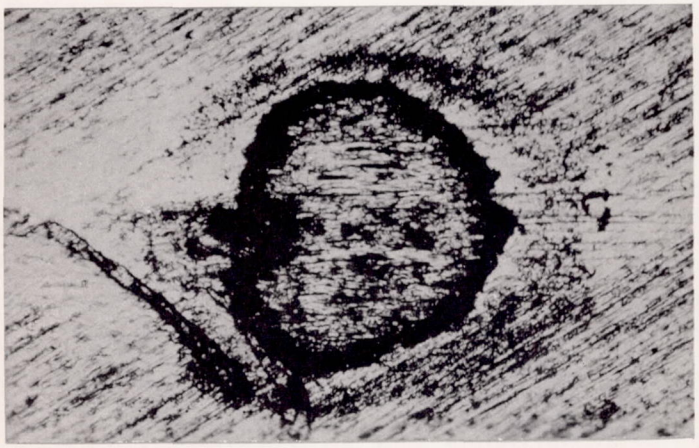

(c) Aluminum-alloy flat after test in vacuum. Before wiping.

Figure 10.- Aluminum-alloy flat run against aluminum hemisphere in air and vacuum. Magnified 100 times.

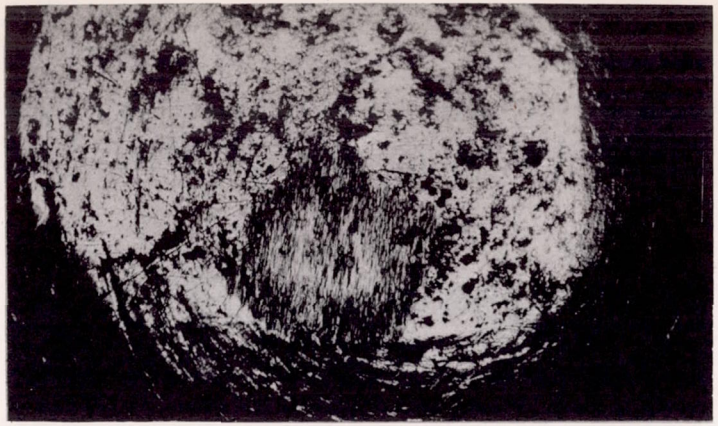

(a) Lead hemisphere after test in air of atmospheric pressure.

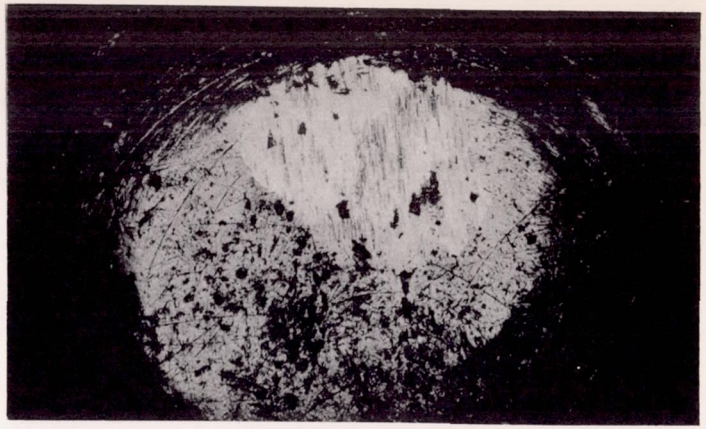

(b) Lead hemisphere after test in vacuum. Wear spot highly polished.

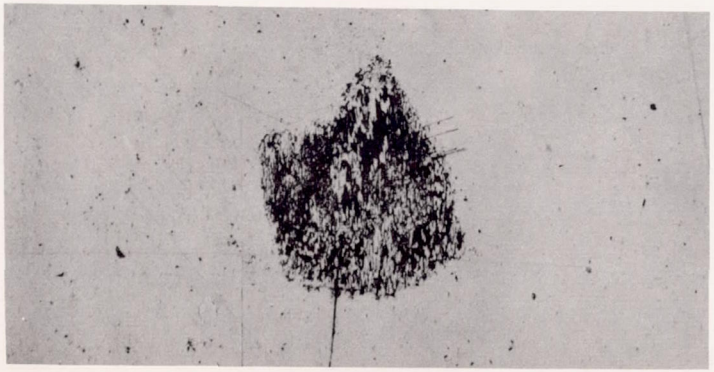

(c) Steel flat after test in air.

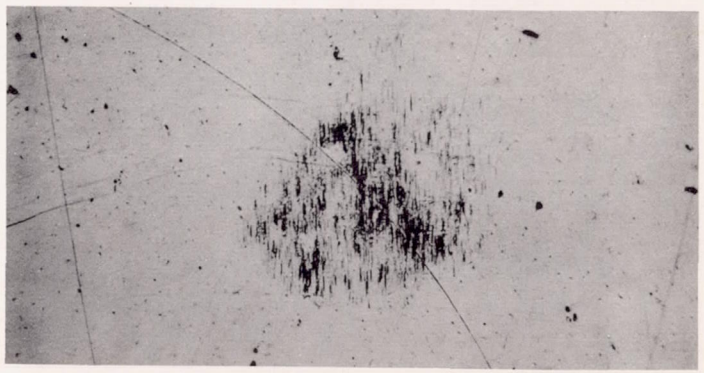

(d) Steel flat after test in vacuum.

Figure 11.- Lead hemisphere run against SAE 1020 steel flat in air and vacuum. Magnified 50 times.

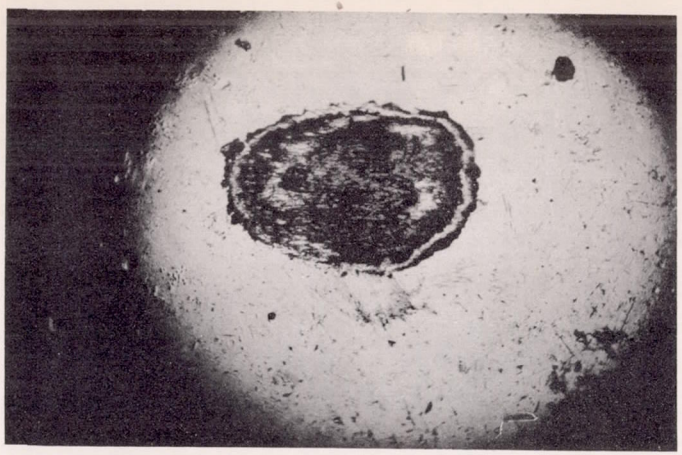

(a) Steel sphere after test in air.

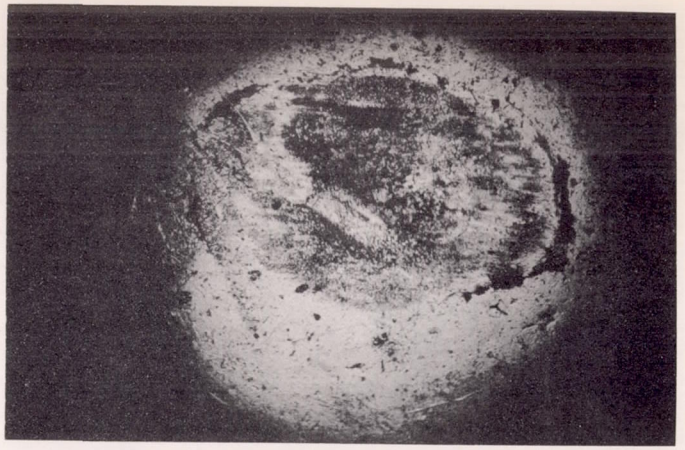

(b) Steel sphere after test in vacuum.

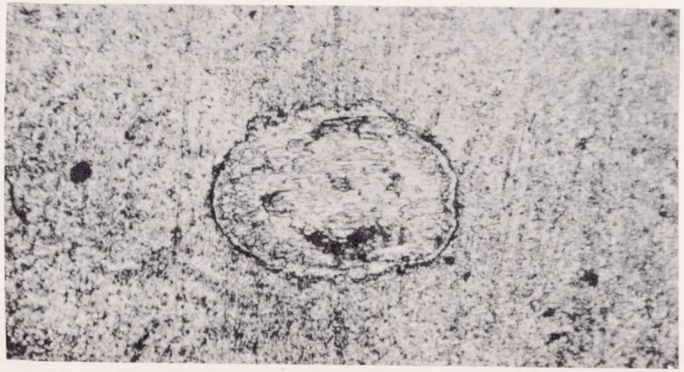

(c) Lead-plated steel flat after test in air.

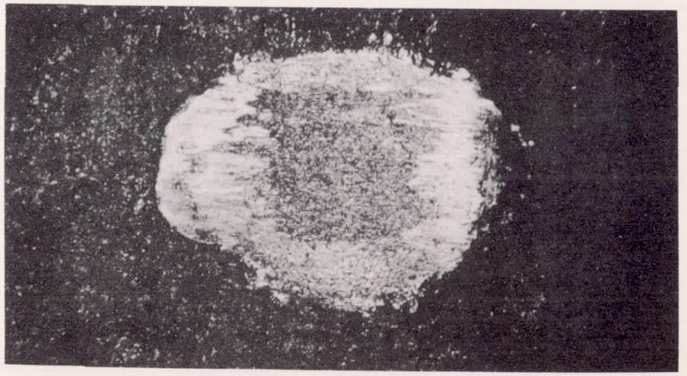

(d) Lead-plated steel flat after test in vacuum.

Figure 12.- Steel sphere run against lead-plated steel flat in air and vacuum. Magnified 50 times.

(a) Steel sphere after test in air. Corroded spot looks brownish.

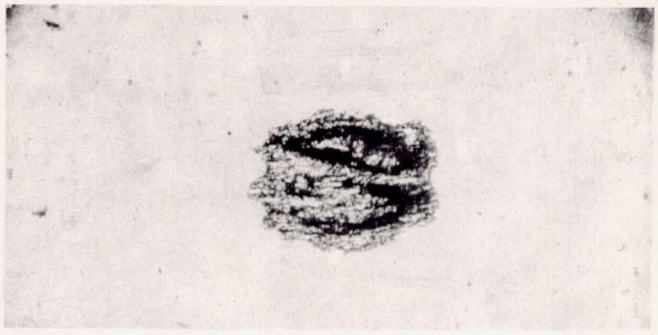

(b) Steel sphere after test in vacuum.

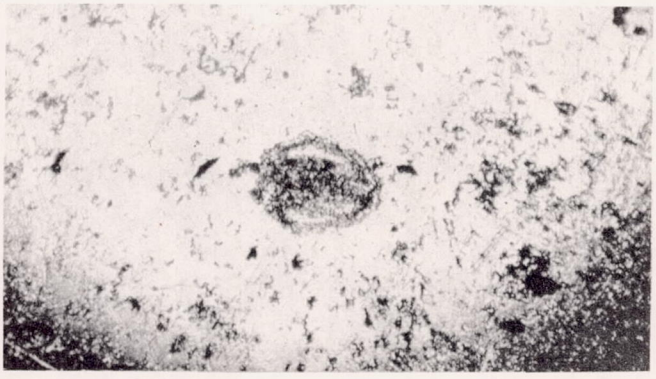

(c) Steel sphere after test in vacuum with degassed specimens.

Figure 13.- Steel against steel in air and vacuum. Chromium-steel sphere against SAE 1020 steel flat. Magnified 100 times. Mating steel flats are shown in figure 14.

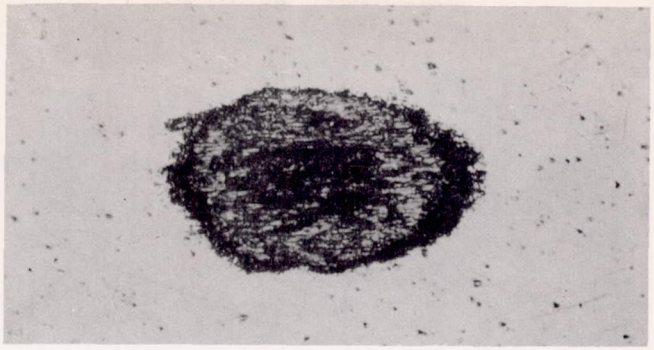

(a) Steel flat after test in air. Corroded spot looks brownish.

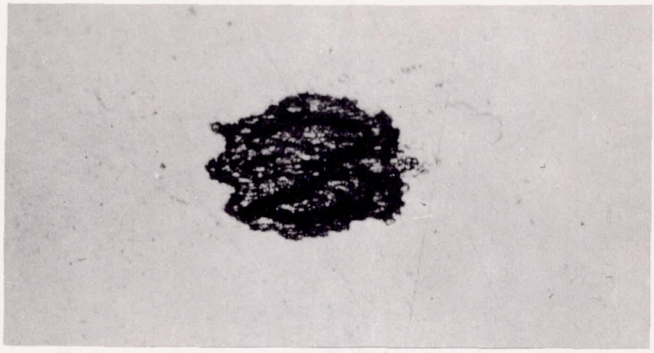

(b) Steel flat after test in vacuum.

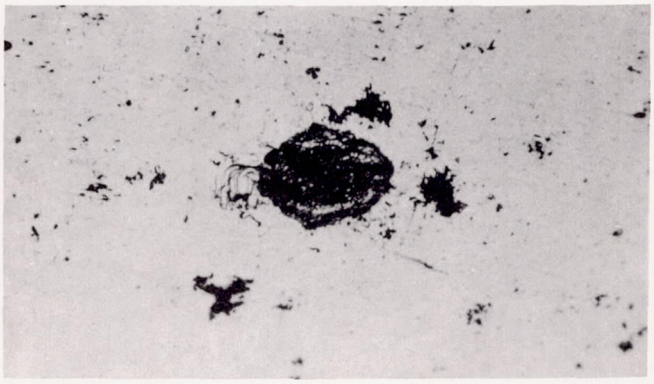

(c) Steel flat after test in vacuum with degassed specimens.

Figure 14.- Steel against steel in air and vacuum. SAE 1020 steel flat against chromium-steel sphere. Magnified 100 times. Mating chromium-steel spheres are shown in figure 13.

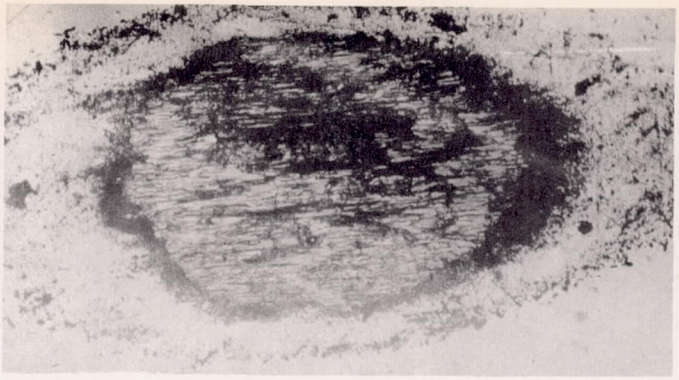

(a) Steel sphere after test in air. Corroded region looks brownish. Magnified 150 times.

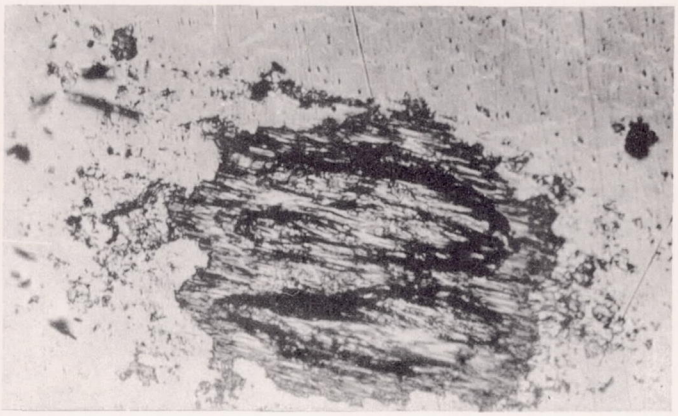

(b) Steel sphere after test in vacuum. Magnified 200 times.

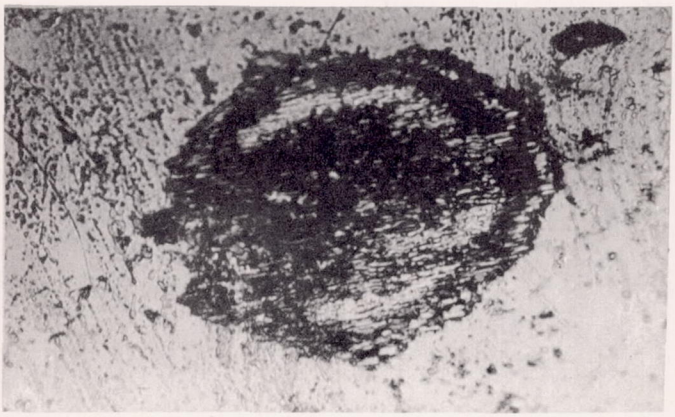

(c) Steel sphere after test in vacuum with degassed specimens. Magnified 300 times.

Figure 15.- Steel against steel in air and vacuum. Chromium-steel sphere against SAE 1020 steel flat. Magnified 150, 200, and 300 times.

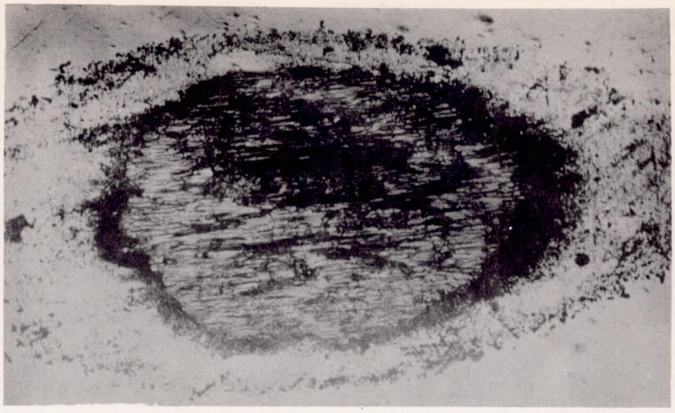

(a) Steel flat after test in air. Corroded spot looks brownish. Magnified 150 times.

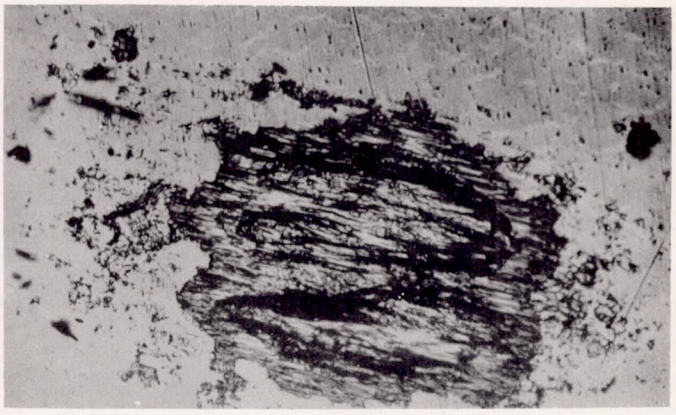

(b) Steel flat after test in vacuum. Magnified 200 times.

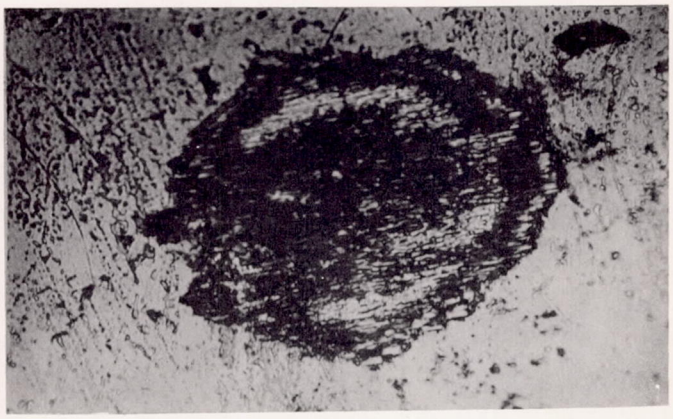

(c) Steel flat after test in vacuum with degassed specimens. Magnified 300 times.

Figure 16.- Steel against steel in air and vacuum. SAE 1020 steel flat against chromium-steel sphere. Magnified 150, 200, and 300 times.

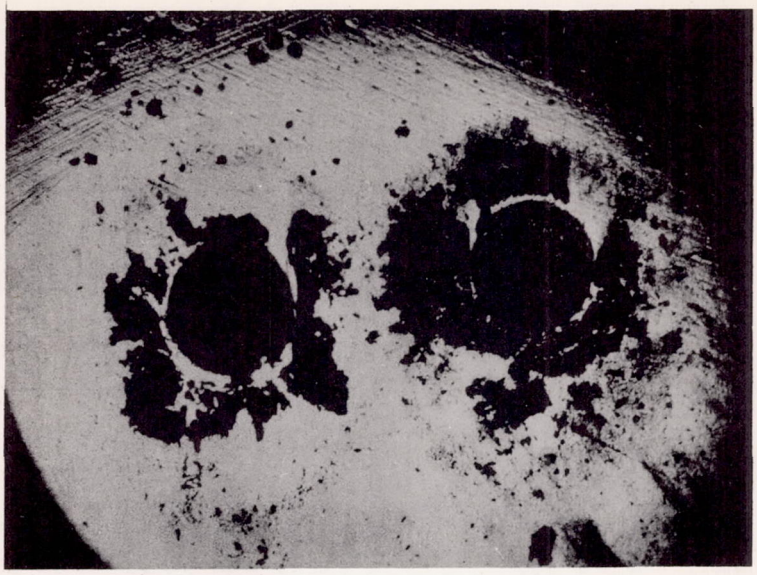

(a) Steel flat before wiping. Right-hand spot is result of corrosion test in air.

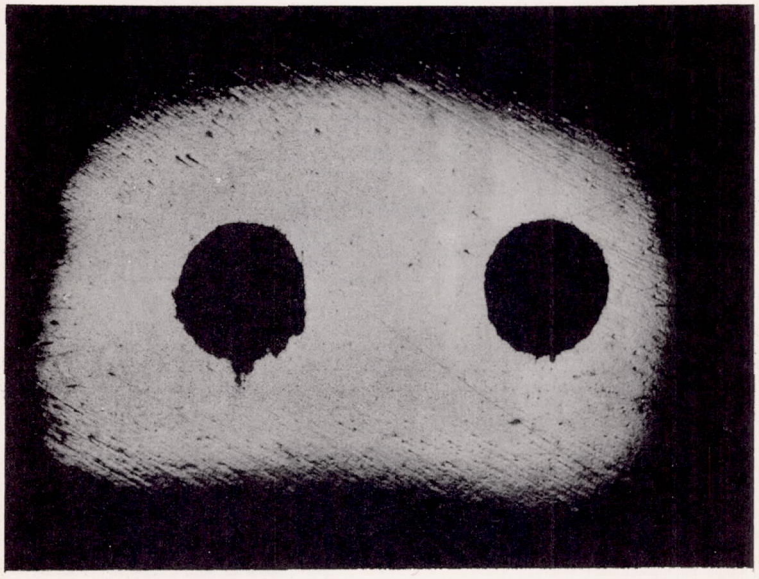

(b) Steel flat after wiping.

Figure 17.- SAE 1020 steel flat run against chromium-steel sphere in oxygen and air of atmospheric pressure. Magnified 25 times.

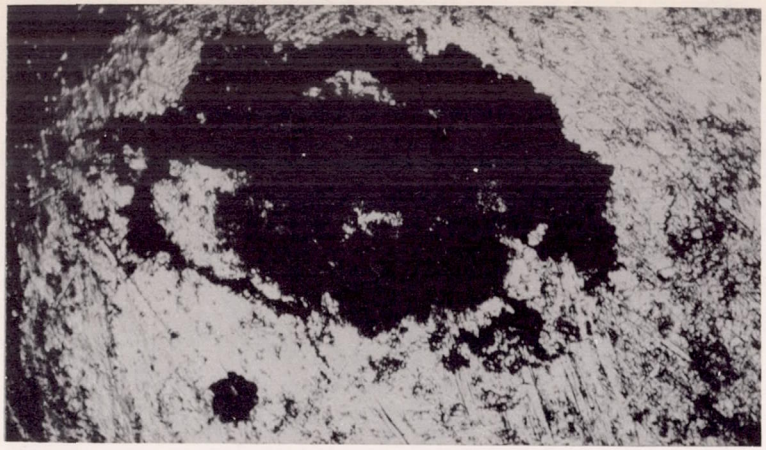

(a) Aluminum hemisphere after test in air. Before wiping.

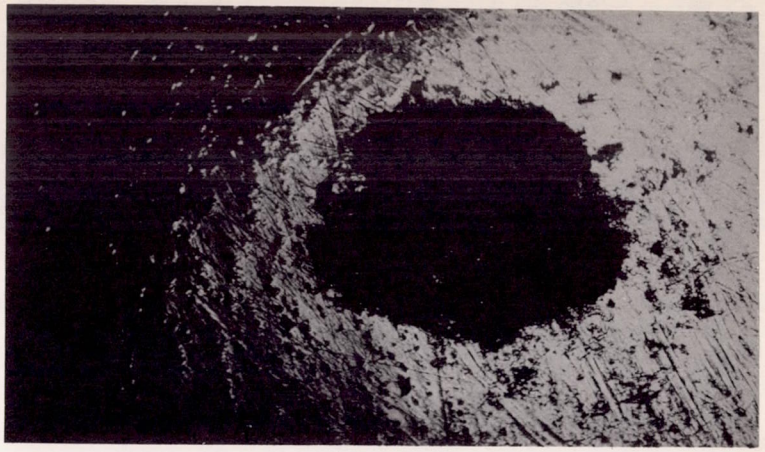

(b) Aluminum hemisphere after test in air. After wiping.

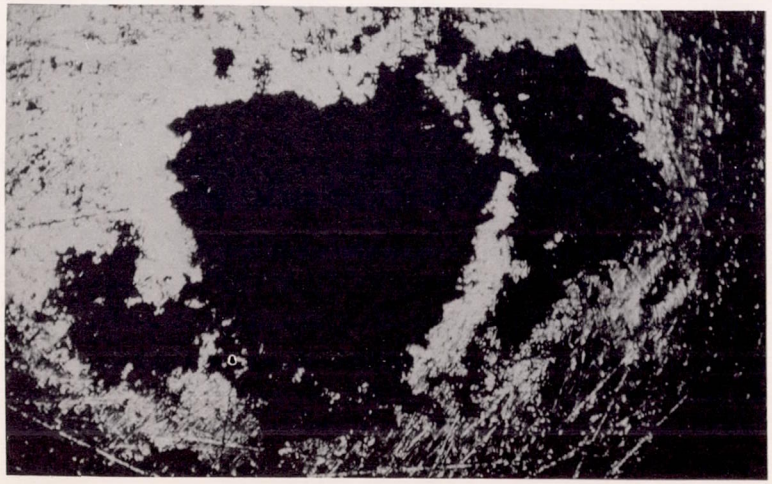

(c) Aluminum hemisphere after test in oxygen. Before wiping.

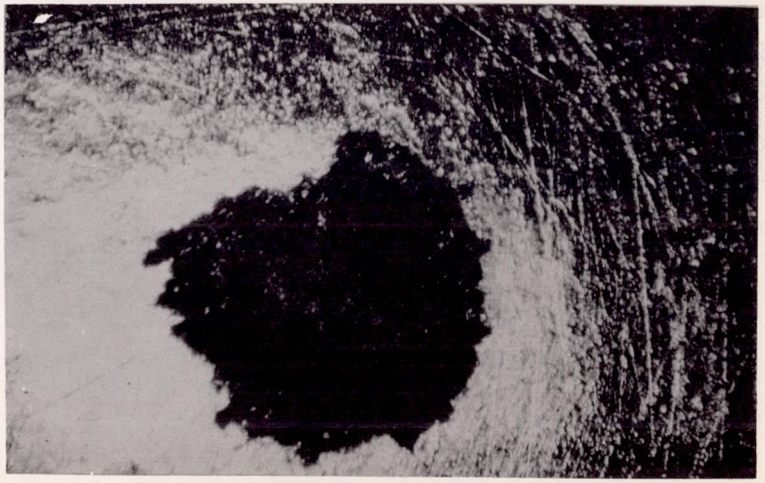

(d) Aluminum hemisphere after test in oxygen. After wiping.

Figure 18.- Aluminum hemisphere run against aluminum-alloy flat in air and oxygen of atmospheric pressure. Magnified 100 times.

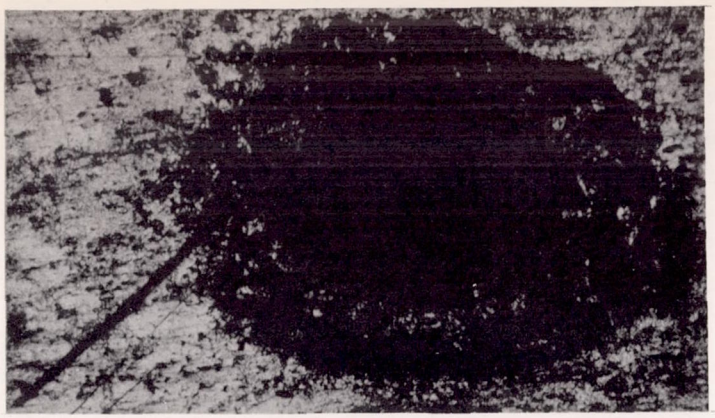

(a) Aluminum-alloy flat after test in air. Before wiping.

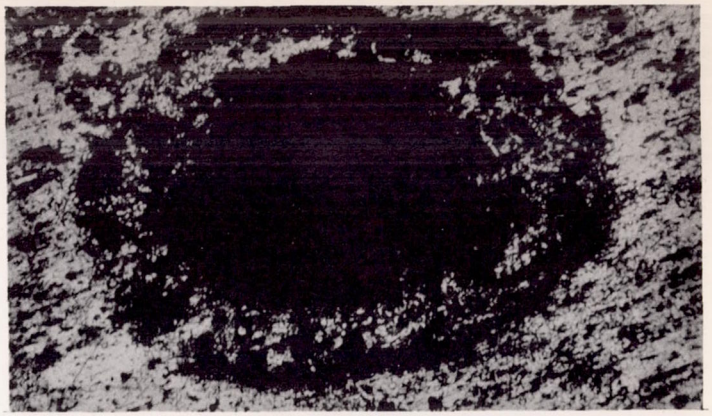

(b) Aluminum-alloy flat after test in air. After wiping. Not all debris was removed by wiping with lens paper.

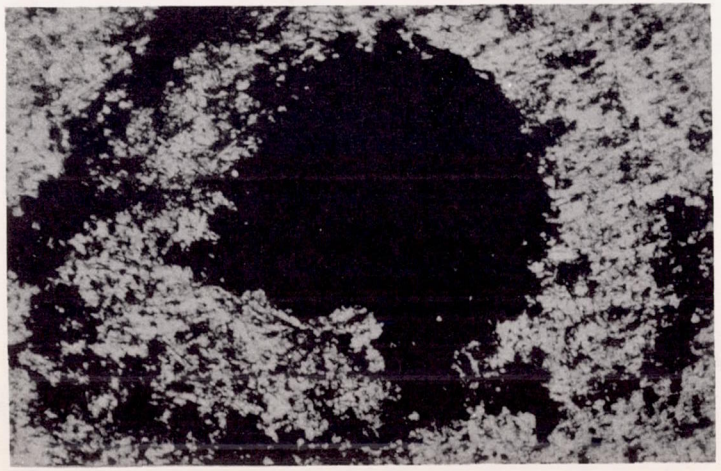

(c) Aluminum-alloy flat after test in oxygen. Before wiping.

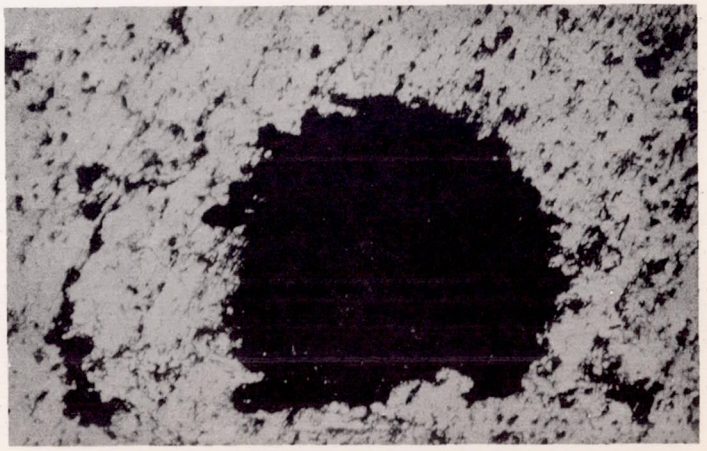

(d) Aluminum-alloy flat after test in oxygen. After wiping.

Figure 19.- Aluminum-alloy flat run against aluminum hemisphere in air and oxygen of atmospheric pressure. Magnified 100 times.

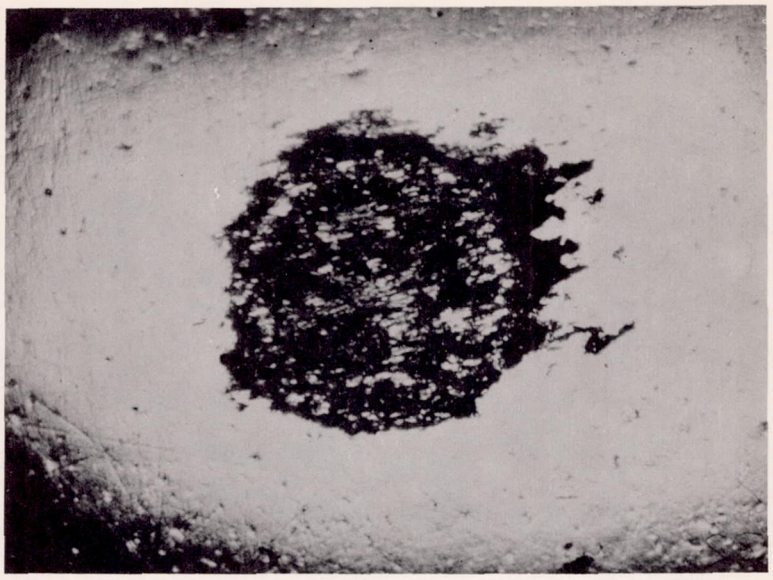

(a) Steel sphere after test in air. Before wiping. Most of the debris is on steel flat.

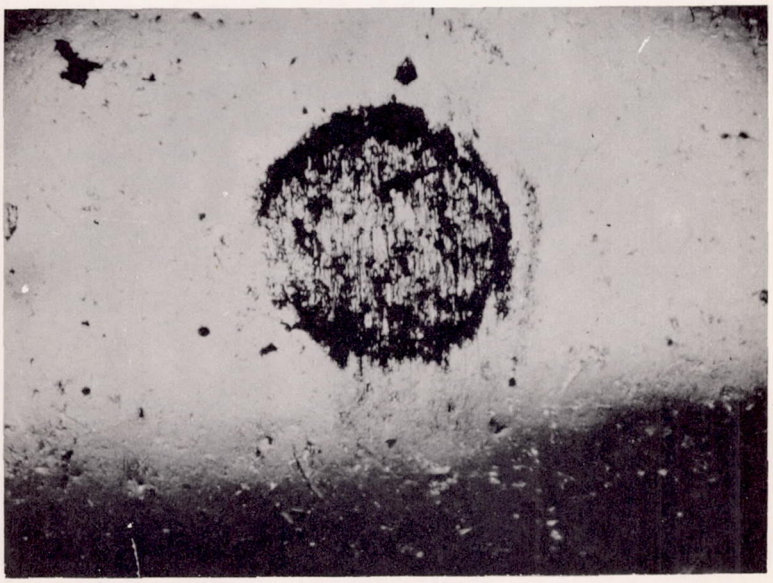

(b) Steel sphere after test in helium. Before wiping. Most of the debris is on steel flat.

Figure 20.- Chromium-steel sphere run against SAE 1020 steel flat in air and helium of atmospheric pressure. Magnified 100 times.

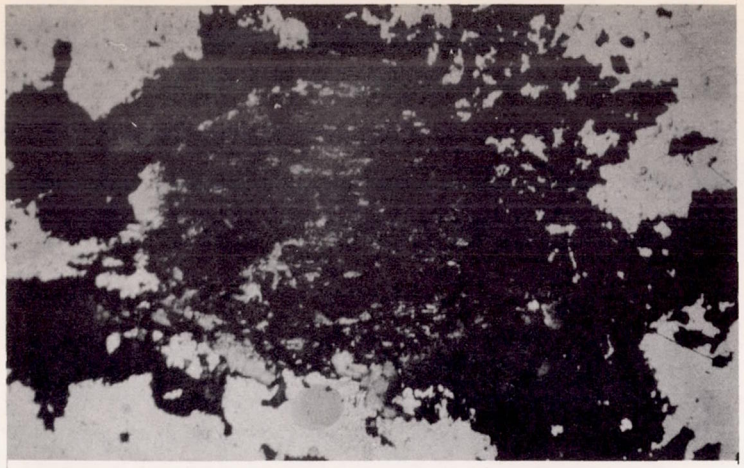

(a) Steel flat after test in air. Before wiping.

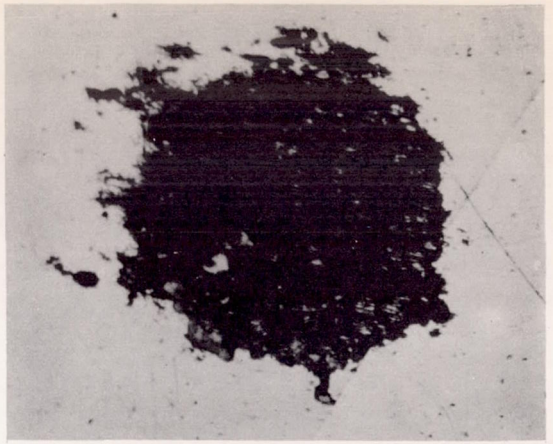

(b) Steel flat after test in air. After wiping.

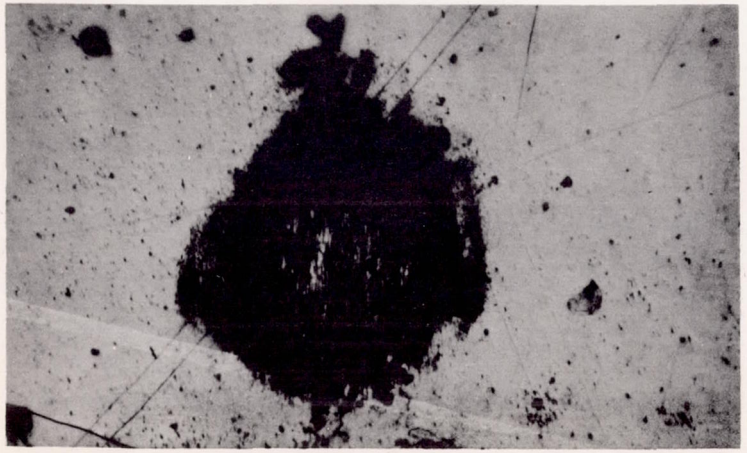

(c) Steel flat after test in helium. Before wiping.

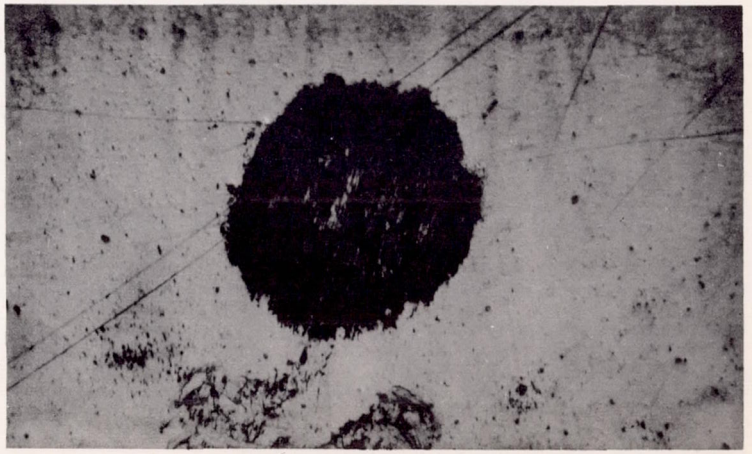

(d) Steel flat after test in helium. After wiping.

Figure 21.- SAE 1020 steel flat run against chromium-steel ball in air and helium of atmospheric pressure. Magnified 100 times.